

# Review of recent advances in segmentation of the breast boundary and the pectoral muscle in mammograms

Mario Mustra<sup>1</sup> · Mislav Grgic<sup>1</sup> · Rangaraj M. Rangayyan<sup>2</sup>

Received: 14 November 2014 / Accepted: 19 October 2015  
© International Federation for Medical and Biological Engineering 2015

**Abstract** This paper presents a review of recent advances in the development of methods for segmentation of the breast boundary and the pectoral muscle in mammograms. Regardless of improvement of imaging technology, accurate segmentation of the breast boundary and detection of the pectoral muscle are still challenging tasks for image processing algorithms. In this paper, we discuss problems related to mammographic image preprocessing and accurate segmentation. We review specific methods that were commonly used in most of the techniques proposed for segmentation of mammograms and discuss their advantages and disadvantages. Comparative analysis of the methods reported on is made difficult by variations in the datasets and procedures of evaluation used by the authors. We attempt to overcome some of these limitations by trying to compare methods which used the same dataset and have some similarities in approaches to the breast boundary segmentation and detection of the pectoral muscle. In this paper, we will address the most often used methods for segmentation such as thresholding, morphology, region growing, active contours, and wavelet filtering. These methods, or their combinations, are the ones most used in the last decade by the majority of work published in this image processing domain.

**Keywords** Mammography · Segmentation · Breast boundary · Pectoral muscle

---

✉ Mario Mustra  
mario.mustra@fer.hr

<sup>1</sup> Faculty of Electrical Engineering and Computing, University of Zagreb, Zagreb, Croatia

<sup>2</sup> Schulich School of Engineering, University of Calgary, Calgary, AB, Canada

## 1 Introduction

Breast cancer has been one of the major diseases affecting women over the past several decades. Mammographic screening has become a standard medical examination and screening tool for women of age 50 years and above. The successful implementation of breast cancer screening programs around the world has greatly increased the number of mammograms that need to be examined, and has created the need for systems for computer-aided diagnosis (CAD) to assist radiologists.

Mammography imaging is X-ray imaging of the breast, and using X-rays as the base technology makes mammography distinct from other imaging techniques. Mammograms are usually high-resolution images with high bit-depth, which provides the possibility of discovering abnormalities masked by surrounding and overlapping breast tissue. CAD systems should include multiple different possibilities for image enhancement, automatic segmentation, and registration, and, in the ideal scenario, automatic detection algorithms for various possible features that could indicate an abnormality. The main preprocessing technique in CAD applications is defining the proper region of interest which implies some sort of image segmentation and object detection. After the segmentation, the user of a CAD system can start all other automatic detection and diagnosis tools on the way to bring a reliable and quick diagnosis.

There are two commonly used ways of capturing and storing mammograms: analog screen-film mammography (SFM) and full-field digital mammography (FFDM). Each of these methods has its advantages, but there is no significant difference in their diagnostic accuracy [28]. FFDM is being used more commonly now because of the convenience of digital storage and lower running cost for each

examination. Even though there is a standard for image storage for use with several medical imaging modalities called DICOM [40], different equipment manufacturers have different storage options because of varying capabilities of the equipment.

In this paper, we deal with image processing techniques for segmentation of the breast tissue from the background in both FFDM and digitized SFM images, and also for segmentation of the pectoral muscle from mediolateral oblique (MLO) mammograms. Segmentation of the breast tissue from the background is important for automatic detection and registration methods as well as for determining the breast tissue boundaries for proper image display without manual adjustment. In MLO mammograms, a part of the pectoral muscle is visible, and obtaining its boundaries leads to useful information about the position of the breast and its orientation as well as the overall intensity of the gray levels in the image. Because of these reasons, many automatic methods for detection of the pectoral muscle and its masking have been proposed, and such methods have become a part of commercial CAD systems. In this paper, we review recent advances in segmentation techniques, with emphasis on the most commonly used approaches that have provided the best results.

It is a challenging task to compare the performance of different methods when they were tested on images from different sources in the initial works because image properties can vary and some techniques can lead to better results when certain types of images are used for testing. It would be ideal to compare all of the methods using the same set of images containing a large selection of images with varying quality and from multiple image capturing sources. There are a few different public mammographic image datasets available, but the most widely used databases are the Mammographic Image Analysis Society (MIAS) database [50] with 322 MLO mammograms and Digital Database of Screening Mammograms (DDSM) [20] with 2620 cases and almost 10,500 both CC and MLO mammograms. These two databases consist of digitized SFM images, which makes them outdated. Unfortunately, no comparable and comprehensive database of FFDM images is publicly available at present. Some of the reviewed algorithms for segmentation of the breast tissue from the background and the pectoral muscle have been implemented in CAD solutions among with nipple detection algorithms, but the information about which commercial software developer uses which algorithm is confidential and not publicly available.

The paper is organized as follows. Section 2 provides descriptions of methods for breast segmentation from the background. Section 3 presents a review of methods for segmentation of the pectoral muscle in MLO mammograms. Section 4 summarizes the most commonly used

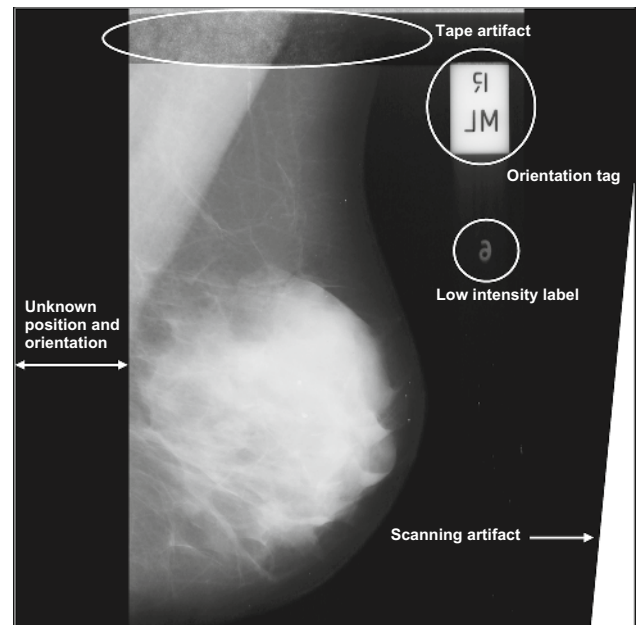


**Fig. 1** Example of an SFM image which contains many background objects and artifacts

segmentation approaches and provides comparative analysis of their results, and Sect. 5 draws the conclusion.

## 2 Segmentation of the breast from the background

Image segmentation is an important initial step in computer-aided analysis of mammograms regardless of the subsequent steps of processing. In the case of scanned SFM images, each image before the segmentation process may contain many objects and artifacts that need to be removed, such as labels, markers, scratches, and, in the worst case, even adhesive tapes. Another important problem that needs to be addressed in the case of scanned SFMs is the orientation of the image and the separation of the breast tissue region from the edge (first column) of the image. Figure 1 shows an example of a scanned SFM image from the MIAS database that contains many background objects and artifacts.

Mammograms are projection images of 3D structures in the breast that have different physical dimensions and cause different levels of attenuation of X-rays. For this reason, similar intensities in the resulting image could be the result of many overlapping tissues of low density or of a few tissues of higher attenuation. Therefore, using solely the intensity in the image cannot guarantee proper segmentation of the desired tissue. There have been many solutions proposed for segmentation of breast tissue from the

background in mammograms, some of which are reviewed in the following paragraphs.

There are many ways to define how accurate an automatic segmentation is, and one of the mostly used approaches is thorough completeness and correctness. Completeness and correctness can be defined using TP, FN, and FP parameters. TP is the true-positive area or area identified correctly by the method; FN is the false-negative area or area missed by the method; and FP is the false-positive area or area identified as error by the method. Completeness and correctness are defined as:

$$\text{completeness} = \frac{\text{area}_{\text{matched}}}{\text{area}_{\text{mask}}} \approx \frac{\text{TP}}{\text{TP} + \text{FN}} \quad \text{and} \quad (1)$$

$$\text{correctness} = \frac{\text{area}_{\text{matched}}}{\text{area}_{\text{segmented}}} \approx \frac{\text{TP}}{\text{TP} + \text{FP}}, \quad (2)$$

where  $\text{area}_{\text{matched}}$  is the area that is common between  $\text{area}_{\text{segmented}}$  as provided by the segmentation method and  $\text{area}_{\text{mask}}$  as provided by the reference or ground truth annotated by an expert.

Qi and Head [43] conducted a study on breast asymmetry with images obtained using a thermal (infrared) camera. Infrared images have different properties in terms of intensity distribution as compared to X-ray mammograms. It is interesting to note that, even though the image modality is different, a few basic preprocessing techniques are used to achieve image segmentation as in images from other modalities. Qi and Head [43] used the Canny edge detector to obtain binary edge images and the Hough transform to extract feature curves which were used to detect asymmetry. The thermograms they used have much lower contrast than mammograms and, therefore, are more difficult to segment because a region of interest (ROI) may be placed differently in each image.

Van Engeland et al. [55] presented a comparison of methods for registration of mammograms with the aim of detecting corresponding areas in the left and right breasts. To segment the breast tissue from the background, they used the low-intensity property of a mammogram's background and morphological operations for removing possibly existing labels. The process for alignment involved detection of the pectoral muscle and detection of the nipple position, which required accurate segmentation of the breast skin-line because the nipple is assumed to be located at the skin-air interface. Hong and Brady [21] used a topographic approach by determining contours of the same or similar intensity and creating an isolevel contour map. A problem with the process for contour creation is the existence of noise; therefore, it is necessary to remove the noise and insignificant details without degrading the edges. For this purpose, Hong and Brady [21] used the anisotropic diffusion filter [58]. Their approach detected regions

corresponding to the breast boundary, the pectoral muscle, masses in general, and dense tissue regions. Although the results of mass detection using 48 mammograms were good, the segmentation accuracy needs improvement according to the results presented in their paper.

Wirth and Stapinski [60] used active contours, also known as snakes, for segmentation of the breast tissue region in mammograms. Active contours are generally sensitive to the seed point location or position of the initial contour and to undesired local intensity minima which can lead to false segmentation. To overcome these problems, Wirth and Stapinski [60] adapted their method to be semi-automatic, with the need to place the initial contour close to the expected result. The proposed method was tested on mammograms from the MIAS database, and the results of only a few cases were shown. Therefore, it is not possible to obtain information about the performance of the proposed method on the entire database, which contains many difficult-to-process images. Wirth et al. [61] proposed a fuzzy segmentation method which uses a combination of two variables, a measure of the size of deviations in a neighborhood surrounding the pixel being processed and a measure of edge sharpness in a neighborhood of the pixel. Evaluation of the method was performed on 120 mammograms from the MIAS database, achieving a result of completeness of 0.99 and correctness of 0.98.

Active contours were also used by Ferrari et al. [16] as a segmentation tool for identification of the breast boundary. As the first step, they performed contrast enhancement of the tissue near the boundary using a logarithmic operation:

$$G(x, y) = \log [1 + I(x, y)], \quad (3)$$

where  $G(x, y)$  is the intensity of the transformed image and  $I(x, y)$  is the input image at the position  $(x, y)$ . After contrast enhancement, their procedure included steps of binarization using the Lloyd-Max quantizer and morphological opening to remove small objects outside the breast region. An approximate breast boundary was extracted from the binary mask using the chain-code method. By observing the intensity variation in pixels along normals to the breast boundary, they extracted an improved estimate of the boundary based on histogram analysis. Furthermore, since the traditional active contour model did not give satisfactory results, they proposed an adaptive active deformable contour model, with which they were able to obtain a more accurate breast boundary, especially in situations when objects of high intensity were present close to the breast boundary. The method was tested on 84 mammograms from the mini-MIAS database and produced the following FP and false-negative (FN) percentages with the corresponding standard deviation:  $0.41 \pm 0.25 \%$  and  $0.58 \pm 0.67 \%$ . An example of accurate segmentation of a mammogram with a label close to the skin-line is shown in Fig. 2.

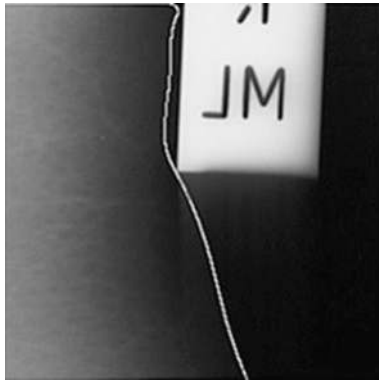


**Fig. 2** Accurate segmentation of the mammogram with a label close to the skin-line [16]

Rickard et al. [45] presented a multiscale analysis method that considers multiple versions of the original image filtered by Gaussian filters with different standard deviation values. Features were obtained by convolving the filtered images with combinations of the derivative of Gaussian function. Self-organizing maps were used in the feature reduction process. The method was tested on 400 mammograms from the DDSM including both craniocaudal (CC) and MLO projections. Based on visual inspection of the results, the authors indicated that the results vary with the use of different numbers of clusters and threshold levels for different breast density categories, but did not provide detailed explanation of the results obtained.

Breast density is a measure or category, indicating the amount or proportion of fibroglandular tissue present in the breast or as seen in a given mammogram. Figure 3 shows examples of four mammograms, one for each category according to the BI-RADS nomenclature [2].

As mentioned earlier, the performance of a method for segmentation is largely influenced by the quality of the given image and contrast of the tissue against the background. Breast density can, therefore, have a large influence on the results of segmentation because of substantial variation in contrast and texture in different categories of density. Different mammographic databases contain images of different properties in terms of spatial resolution, bit-depth, presence of artifacts, and breast density categories. Visual differences between mammograms from different databases are illustrated in Fig. 4. Problems related to these issues were studied by Wirth et al. [62], who also mention the problem of demonstrating acceptable performance of segmentation algorithms in mammography.

Besides the properties of a given image, another aspect that should be taken into account is the difficulty to segment a certain mammogram. In the segmentation step, most algorithms use the same property to distinguish breast tissue from the background, based on differences

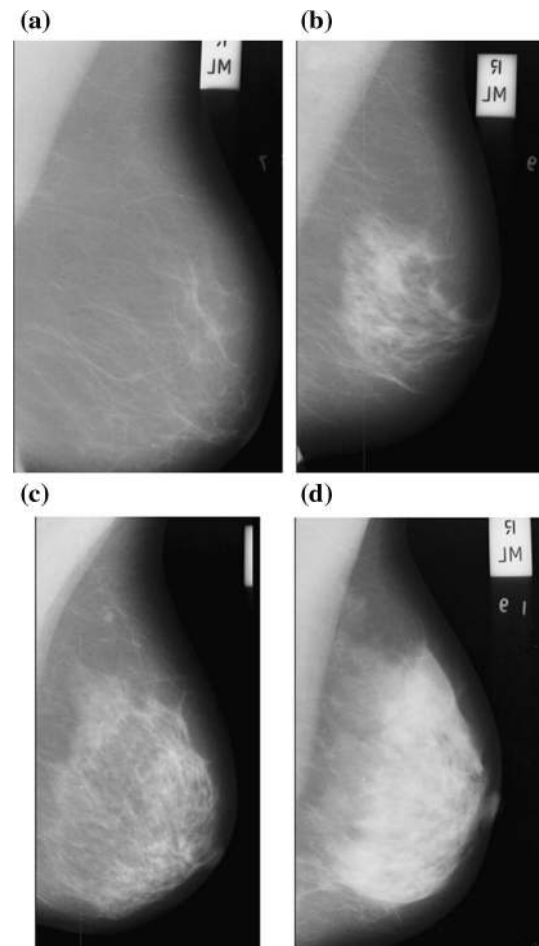


**Fig. 3** a–d Mammograms belonging to BI-RADS I to BI-RADS IV, respectively

in local or global intensity. The difference between various approaches is in finding other important properties and combining their results to achieve an accurate decision as to whether the pixel being analyzed belongs to the class of breast tissue or to the background. The problem of sensitivity to the variation in intensity and accuracy in segmentation with a “difficult” mammogram “mdb006,” which has a bright label close to the breast tissue, is shown in Fig. 5 from Wirth et al. [62].

The questions that arise after observing Fig. 5 are “What is the acceptable accuracy of an automatic segmentation algorithm?” and “Is there a rule that would assist in making a decision as to whether the accuracy of segmentation is adequate for a CAD system?” Unfortunately, there is no mathematical procedure that can answer these questions, and the benchmark to assess the accuracy of segmentation is manual evaluation by an expert radiologist.

Baker et al. [4] conducted a study on the accuracy of segmentation of a commercial CAD system for mammography. Their results, obtained by manual evaluation of

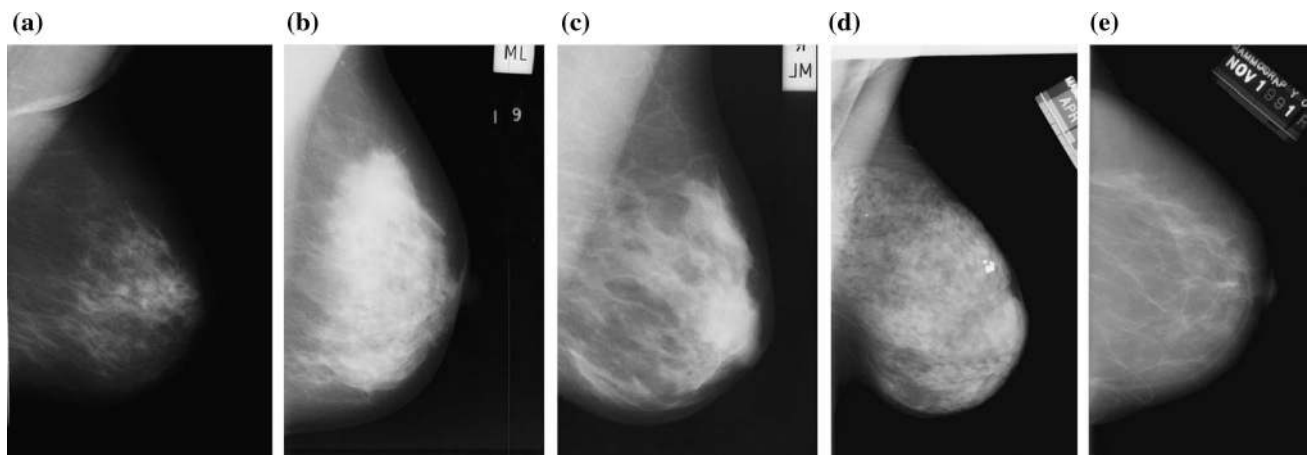


**Fig. 4** **a** Mammogram from the Nijmegen database; **b, c** mammograms from the MIAS database; **d, e** mammograms from the DDSM database [62]

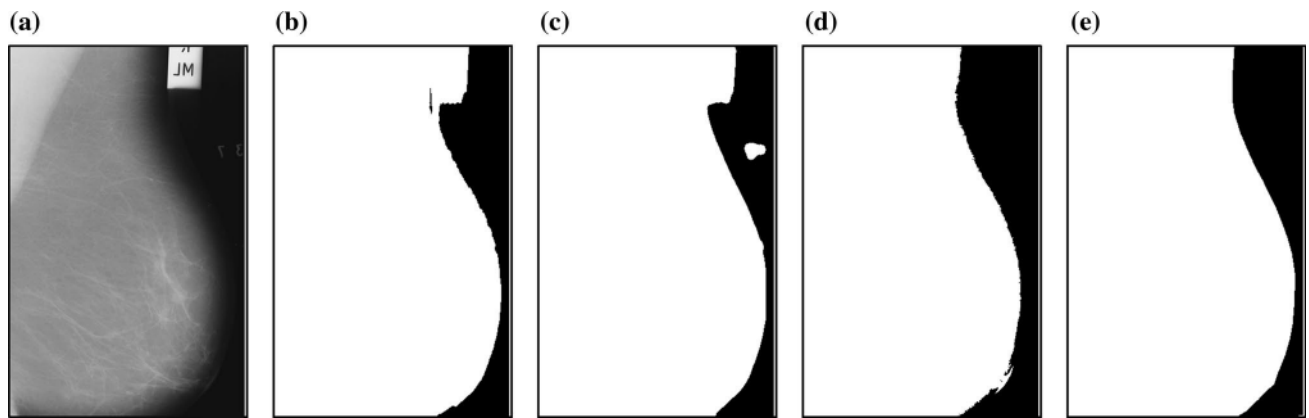


**Fig. 5** **a** Original mammogram “mdb006” from the MIAS database; **b** segmentation mask using polynomial modeling; **c** segmentation mask using fuzzy-rule-based segmentation; **d** segmentation mask using knowledge-based segmentation; **e** ground truth segmentation [62]

segmented images, gave the result of 96.8 % of near perfect or acceptable segmentation of 2020 mammograms from 507 women. The tested images were both SFMs and FFDMs obtained from a direct conversion mammographic device with the spatial resolution of 50  $\mu\text{m}/\text{pixel}$ . Wei et al. [57] used a global thresholding method and morphological operations for segmentation of the breast boundary from the background. They used the watershed transform, which combines region growing and edge detection techniques, on the edge region of the breast tissue to detect the actual edge. The results of the proposed method show 94.9 % of accurate segmentation; ad problems in the segmentation accuracy occurred in cases of oversized breast tissue regions in the mammogram. Raba et al. [44] proposed a method for breast tissue segmentation that uses an adaptive histogram approach and selective region growing for removal of the pectoral muscle. Different thresholds were set, and masks calculated using the thresholds were overlapped. The

regions defined by the boundary of the smallest threshold to the boundary of the largest one were statistically evaluated to calculate the mean gray level for use as the final threshold value. To test the proposed method, they used the mini-MIAS database, which contains same images as the original MIAS database but with reduced size and spatial resolution of 200  $\mu\text{m}/\text{pixel}$ . The proposed method resulted in 98 % of accurate segmentation. Besides detection of the breast boundary itself, the proposed method also provides the possibility to detect a few key points on the boundary, such as the nipple location.

An approach that relies on detection of the stroma edge and extrapolation of the breast skin-line from the stroma was presented by Sun et al. [52]. Stroma is the tissue between the ducts and glands in the breast composed of fat and fibrous tissue in varying proportions. Figure 6 depicts the stroma edge and the skin-line in an MLO mammogram [52].

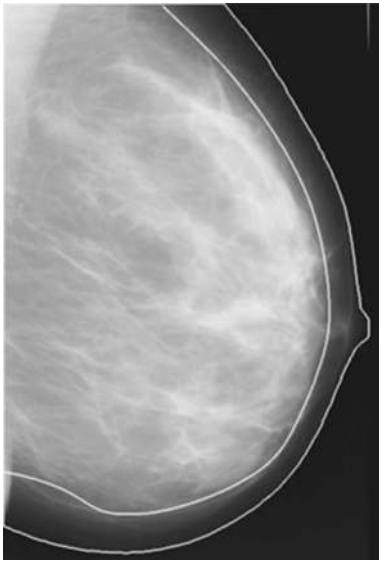


**Fig. 6** Stroma edge and the skin-line in a MLO mammogram [52]

The stroma edge usually has high contrast with respect to the mostly fatty tissue near the breast border, and is seen as a dark region not only because of its type but also because of its physical dimensions, which are smaller and therefore present lower attenuation for X-rays. For these reasons, Sun et al. [52] used Otsu's thresholding method. For detection of the initial segmentation contour, they relied on the property that the stroma of the breast has more or less a uniform distance to the breast skin-line. For removal of labels and nontissue objects from the background, they used morphological opening and closing operations which also helped in smoothing the breast area. However, the detected edges of both the stroma and the breast tissue were not smooth. To overcome this problem, they used downsampling and neighborhood-averaging with cubic spline fitting. To test their method, Sun et al. used 82 mammograms from the mini-MIAS database. The method resulted in a mean error of 3.28 pixels with standard deviation of 2.17 pixels.

Karnan and Thangavel [24] used a genetic algorithm to detect the breast border and the nipple position. As the first step, they enhanced the original image and removed artifacts and then applied threshold to get the binary image. After that, they extracted the breast border from the breast segmentation mask and then enhance the breast border using the genetic algorithm. The nipple position was determined from the pixels belonging to the breast border using the genetic operators such as reproduction, single-point crossover, and mutation to get new population of strings. Pixels which generated the minimum value of a fitness measure in the genetic algorithm are treated to be the nipple position. By knowing the breast tissue border and

nipple position, they were able to determine the exact orientation of the image and extract suspicious regions using bilateral subtraction of the left and right mammograms. To test their methods, Karnan and Thangavel used images from the MIAS database, but did not provide information about the success of the methods in terms of segmentation accuracy because their work was aimed at the detection of asymmetry.

Yapa and Harada [65] used the fast marching method that makes possible segmentation of arbitrary shapes. The method starts from a seed point, and the boundary is estimated in each step until the evolved curve describes the actual edge of the breast tissue. This method in the two-dimensional case is similar to region growing with a different interpretation. In the fast marching method, the speed function tries to determine when an edge represented by a sudden intensity change appears. In such a case, a region growing algorithm would reach the stopping criterion in the direction of the edge detected but could continue to propagate in another direction. With the fast marching method, the segmented object remains inside a closed contour, and this approach eliminates false segmentation results due to inconsistencies in the background. The problem that needs to be addressed is "boundary leaking" due to low contrast of the tissue edges toward the background; this was achieved by applying the alternating sequential filter, which is a morphological operation of area closing followed by area opening. The proposed method was tested on 100 images from the mini-MIAS database, and the results obtained for completeness and correctness were 98.6 and 99.1 %, respectively.

Martí et al. [34] used a contour growing approach, which is similar to the active contours approach. The original image was first filtered with a Gaussian smoothing function at different scales, and on the result for each scale, an edge detection algorithm was applied to extract edges. Next, a seed point was detected to start the contour growing process. The initial seed point was obtained as the first local maxima of the gradient in the scale space representation along the  $x$ -axis at half the height of the image. Further refinement was based on analyzing the position of various seed points at close the same position at a small range in the  $y$ -coordinate, and the final seed point was obtained using a least median error estimation. Once the seed point was detected, a contour growing process starts based on the combination of different criteria. For each point, a set of candidate growing points were obtained situated in a normal line along the gradient direction, and the one which fills the criteria best is chosen to belong to the breast border. Testing of the method was performed on 65 MIAS and 24 DDSM images, and the results were compared with manually segmented images. The results obtained for completeness and correctness were about 0.96 for both measures.

According to the authors' observations, the algorithm faced problems with noisy images which led to poor estimates of the initial seed point and with nonuniform breast intensity distribution which yielded undersegmented images.

Oliver et al. [41] worked on classification of mammographic images based on the amount of fibroglandular tissue. Before the feature extraction process, they needed to have fully segmented breast tissue from the background with the pectoral muscles removed. Since their work was based on tissue type classification, there was no need to use accurate segmentation methods, because a small loss of pixels representing the tissues around the breast border could be neglected in the tissue classification process without much influence on accuracy. For these reasons, they used the method by Raba et al. [44].

A complete system for segmentation of mammograms was proposed by Tzikopoulos et al. [54], including pre-processing, noise estimation, and image filtering, as well as detection of the breast boundary, the pectoral muscle, and the nipple. Images were transformed so that the chest wall location is always on the left side of the image and the pectoral muscle is situated in the top left corner. In the second step, procedures were included to remove objects that did not correspond to breast tissue, such as tape artifacts and labels, with a combination of logical and morphology operators on a thresholded image. To detect the breast tissue boundary, they used the property of the skin–air interface being the smoothest section of identical pixels near the breast edge. In order to estimate the boundary, they relied on polynomial fitting of the pixels from the detected region with orders of 5–10. This procedure was repeated for different threshold values and that producing the least error was selected. No information was provided about the speed of the boundary detection algorithm; use of a procedure for polynomial fitting could demand substantial computational time. Their procedure for detection of the pectoral muscle is described in the following section. Their method for detection of the nipple relies on accurate detection of the region where the nipple should be situated and threshold-based search of the same region with the condition that the nipple is 2–10 mm in size. Results of breast boundary segmentation obtained using the mini-MIAS database were indicated as 0.900 according to the Tanimoto coefficient and 0.945 according to the dice similarity coefficient. The nipple detection method resulted in correct detection for 88 of 118 cases with the nipple being visible in the breast profile.

A threshold-based approach for segmentation of digital mammograms with wavelet-based decomposition for removal of the pectoral muscle was presented by Mustra et al. [38]. Segmentation of the skin-line was performed on digital mammograms preprocessed on the imaging device and enhanced for viewing on the workstation display

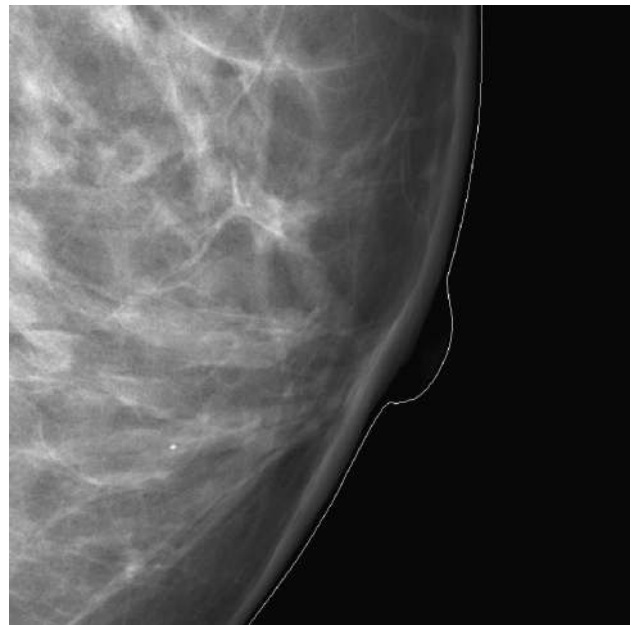


**Fig. 7** Detected breast border contour around *nipple region* [38]

(“for-presentation” category). Because of the preprocessing step, the mammograms have better contrast and do not have labels and artifacts that are usually present in SFMs. Therefore, the process of segmentation of the breast boundary achieved a success rate of 100 %, while segmentation of the pectoral muscle was of acceptable accuracy in 85 % of the cases. An example of accurate segmentation of the breast boundary is shown in Fig. 7.

A method for segmentation using graph-cut techniques was presented by Saidin et al. [46]. This technique requires the user to select a few pixels that belong to the object of interest and a few pixels belonging to the background. The method is designed for segmentation of different tissue types, such as the pectoral muscle, masses, and dense tissue in mammograms, as well as the breast tissue from the background. Since the technique is not completely automatic, user interaction may take substantial time. Nagi et al. [39] proposed a method for breast profile segmentation that uses median filtering to remove noise and small artifacts that can exist in both background and breast tissue. For removal of labels, they used the approach of thresholding combined with morphological operations. To determine which objects are labels, they used an automatic method for counting of pixels that are joined together and create the same object. These steps were performed by image processing functions in the MATLAB Image Processing Toolbox; see Gonzalez et al. [19] for details. After segmentation, their method proceeded with contrast enhancement and removal of the pectoral muscle using a seeded region growing technique. To define the success of the method, they included a step to

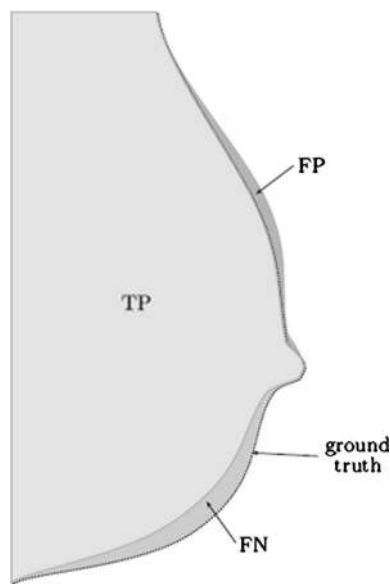


**Fig. 8** Definition of TP, FP, and FN segmentation results according to the ground truth [39]

divide the segmented area into regions of TP, FP, and FN detection by overlapping the segmentation mask with the ground truth segmentation mask drawn by a radiologist; see Fig. 8. Whereas no quantitative results were provided, it was claimed that the segmentation results were of “high accuracy.”

The approach for segmentation of the breast skin-line presented by Zhang et al. [66] used a region growing algorithm with automatic seed detection, morphological operators, and low-pass filtering to smooth the detected boundary. In the method for automatic seed detection, initial seed points are located around the start and end point of the diagonal reference line that goes from the top left to the lower right corner of the image, as shown in Fig. 9.

For removing noise and artifacts, Zhang et al. [66] used a technique known as connected component labeling that finds the largest object in the image and removes all other objects. The final step was smoothing the breast boundary, which was done using a low-pass filter in the frequency domain. To test the proposed method, they used 20 randomly selected images from the mini-MIAS database, and indicated that the results were highly accurate with no quantitative analysis of segmentation accuracy.

The use of statistical properties of mammograms to extract the breast boundary was investigated by Tayel and Mohsen [53]. They used a technique of applying different threshold values for segmentation of regions with similar properties in different images. Adequate explanation of how the thresholds were chosen was not provided. This paper also does not provide quantitative analysis of the success of segmentation, and visual inspection of the

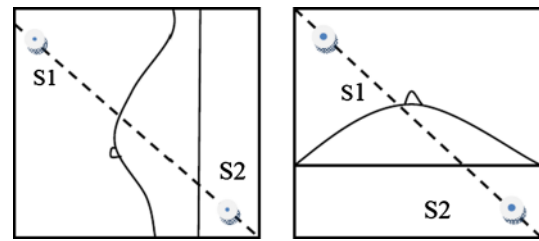


**Fig. 9** Location of two seed points for the region growing

segmentation masks shows that the accuracy of segmentation of details around the breast boundary and the pectoral muscle boundary does not compare favorably with the results of state-of-the-art algorithms.

A statistical approach for segmentation of breast tissue was presented by Oliver et al. [42]. The aim of their work was to determine breast density from mammograms by finding the amount of fibroglandular tissue in the overall breast tissue. Since they used the MIAS database, which contains only MLO mammograms, it was necessary to preprocess the images to remove all the labels from the background as well as the pectoral muscle. For preprocessing, they adopted the method presented by Martí et al. [34]. The approach of Oliver et al. consists of modeling tissue in such a way that image regions are classified according to image patches manually extracted from several images and belonging to various tissue categories. Their method is based on the Karhunen–Loève transform used commonly in face recognition and linear discriminant analysis. The methods provide good accuracy in tissue type categorization but could present problems in segmentation accuracy because the image patches used have limited physical size.

Chen and Zwiggelaar used a combined method for identification of the breast boundary [12]. For an initial approximate threshold, they used the valley between two peaks in the histogram of the image representing the breast tissue and the background. From the resulting binary image, they extracted the largest object that is expected to represent breast tissue using the connected component labeling algorithm. To detect the actual breast edge, they placed 40 points along the detected object’s boundary and performed edge detection on an orthogonal line of width 100 pixels at each of the 40 points. This process was repeated three times using a different Gaussian kernel for filtering. Then, a contour growing method was applied to detect 40 seed points placed one per each line orthogonal to the breast boundary. The new set of points was then used for cubic polynomial fitting to obtain the final breast boundary. The method was tested on the MIAS database and resulted in 64.8 % of accurate, 34.0 % of near accurate, 1.2 % of acceptable, and 0 % of unacceptable segmentation. The segmentation accuracy was similar for mammograms from a different



database and slightly worse for segmentation of the pectoral muscle.

Maitra et al. presented a complete preprocessing scheme of digital mammograms [33]. They proposed automatic detection of the orientation of the breast with no information according to the DICOM protocol; mammograms were oriented such that the chest wall is situated on the left border and the pectoral muscle is situated in the top left part of the image. For image enhancement, they used the contrast limited adaptive histogram equalization (CLAHE) technique [67]. No accurate description was provided as to how segmentation was performed after the enhancement step; it could be assumed that a method of thresholding was used. Applied on the mini-MIAS database, the method provided 95.71 % of acceptable segmentation.

Mustra and Grgic [37] proposed a method for segmentation of the breast tissue from the background, designed mainly for scanned SFMs that suffer from background inconsistency and misalignment of images. The proposed method includes removal of tags and background artifacts using morphological opening, which eliminates the influence of nontissue objects in the processes of image alignment and detection of the skin–air interface. After roughly estimating the breast tissue area, a finer thresholding is achieved by dividing the tissue near the skin–air interface into smaller segments, which makes thresholding more accurate. This allows the use of multiple different threshold values and, therefore, more accurate detection of the breast border. In segmentation of SFM images, there is always the problem of smoothing the detected tissue boundary because of uneven intensity of pixels that belong to the corresponding object. To overcome this problem, Mustra and Grgic [37] split the ROI for border detection into smaller ROIs and transformed them from the rectangular to the polar coordinate system. The polar coordinate system was chosen because it represents the shape of a breast boundary better than the rectangular coordinate system, as shown in Fig. 10. The method was tested on the entire mini-MIAS database and resulted in 91.6 % of successfully segmented mammograms, 7.5 % of acceptably segmented mammograms, and 0.9 % of unacceptable segmentation, with the average error in the segmented area equal to 3.7 %.

Casti et al. [10] used Otsu's thresholding method and the Euclidean distance transform with edge detection by means of multidirectional Gabor filtering. To enhance edge visibility, they used an adaptive values-of-interest (VOI) transformation, which gives the result shown in Fig. 11. After VOI transformation, they used 18 Gabor filters and superposition of their responses for each image. Image filtering in this manner produces many edge responses that do not belong to the breast boundary, and therefore, they need to be removed from consideration. By knowing the expected position of the breast boundary, Casti et al. [10] were able

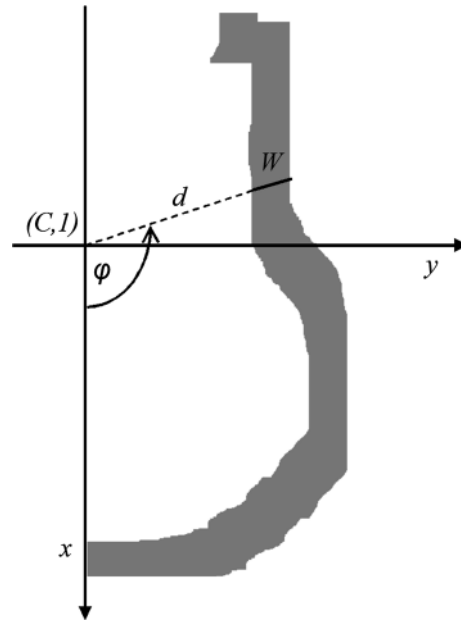


**Fig. 10** ROI for detection of the breast border which has width equal to  $W$  and begins at the distance  $d$  from the origin of a *half-plane* represented in polar coordinates

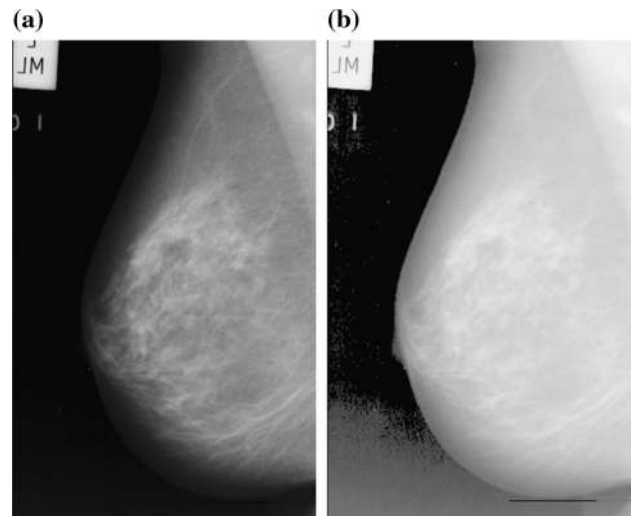


**Fig. 11** **a** Original mammogram “mdb007” from the mini-MIAS database; **b** same mammogram after applying VOI transformation [10]

to remove most of the false edge responses that belong to the background. The final step in creating the breast boundary was edge linking to produce a closed boundary, from which they were able to create a segmentation mask. The method was tested on 249 mammograms from the mini-MIAS database and 194 FFDM images. The results were evaluated using the measures of completeness, correctness, and quality, with quality defined as:

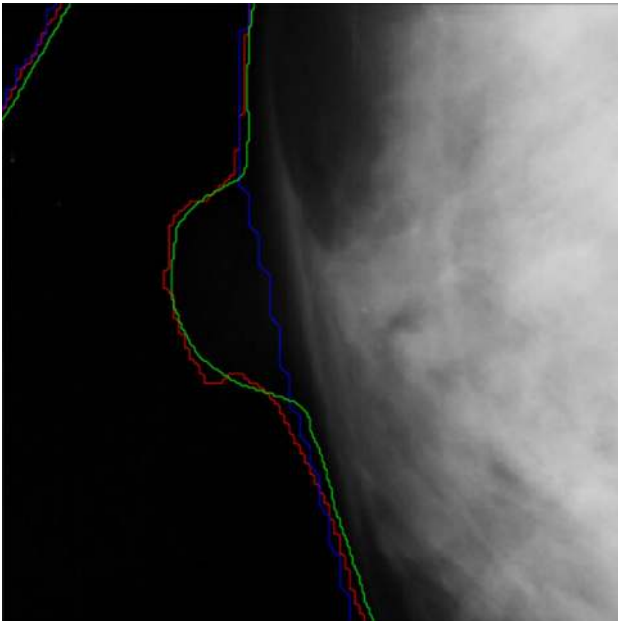


**Fig. 12** Segmentation accuracy where *red line* is the result of method [10], and *green line* shows ideal segmentation (color figure online)

$$\text{quality} = \frac{\text{TP}}{\text{TP} + \text{FP} + \text{FN}} \quad (4)$$

and the values obtained were  $99.87\% \pm 0.003\%$ ,  $99.57\% \pm 0.004\%$ , and  $99.37\% \pm 0.005\%$ , respectively. Figure 12 shows an example of good estimation of the breast boundary around the nipple region.

### 3 Segmentation of the pectoral muscle

Another important step in preprocessing of MLO mammograms is detection of the pectoral muscle. The pectoral muscle is situated on the side of the chest wall, mostly on the upper half of the image, and is usually seen as a brighter region than the rest of the mammogram. The reason for the brighter appearance is that the pectoral muscle causes higher attenuation of the X-rays than breast tissue. Because of this reason, most methods for detection of the pectoral muscle are based on intensity-related properties. Most algorithms search for the edge that represents a decay of intensity toward the breast tissue. There are many different imaging techniques that result in different overall contrast of mammograms, and the appearance of the pectoral muscle is also affected. In Fig. 13a, b, we can observe how mammograms can present different appearance in terms of contrast of the pectoral muscle toward the breast tissue.

Kwok et al. presented a method for estimation of the edge of the pectoral muscle with a straight line [26], which should be adequate for applications where pixels of the

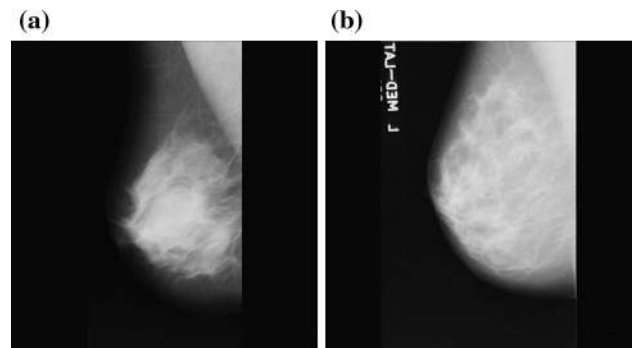


**Fig. 13** **a** Mammogram “mdb001”; **b** mammogram “mdb029,” both from the mini-MIAS database, with different contrast of the pectoral muscle toward the breast tissue

pectoral muscle need to be removed. Whereas it is necessary to know or determine the orientation of the given mammogram, detection of the breast boundary is not required in most methods for the detection of the pectoral muscle. Kwok et al. used iterative thresholding in the area where the pectoral muscle was expected to be located. To detect the exact pectoral muscle border, they used a cliff detection method along the estimated straight line. An area close to the estimated line was filtered using bicubic spline interpolation, the edge detection method was applied, and finally, the region was closed. The method was tested on the MIAS database, and 94 % of images were segmented with acceptable accuracy.

Weidong and Shunren presented a model-based method for segmentation of the pectoral muscle [59]. They used iterative thresholding until the threshold converged to a steady value in a quarter of the given mammogram where the pectoral muscle is expected to be situated, depending on its orientation. A problem that can occur in using this method is due to the uneven size of the pectoral muscle in different mammograms: Use of exactly one-quarter of the given mammogram may not represent the best solution because the iterative procedure is sensitive to the nature and number of the pixels selected, which vary according to size of the actual pectoral muscle. Weidong and Shunren attempted to overcome this problem by using different ROI sizes and choosing one such that a significant number of pixels are properly thresholded in the area where the pectoral muscle in the image is expected to be present. On the binary mask obtained, they used different fitting and line estimation methods, including the Hough transform, twice line fitting for better approach to the exact curvature of the pectoral muscle, and polygonal modeling. The proposed method was tested on 60 mammograms and achieved 81.7 % of accurate segmentation; no information was provided about the database used.

Ferrari et al. [17] proposed a method for automatic detection of the pectoral muscle based on the Hough transform. The Hough transform is commonly used to detect straight lines in an image by converting points or pixel values from the image space into the Hough space. By determining the highest value in an accumulator in the Hough space, it is possible to detect the longest or the brightest line in the image by obtaining information of its distance from the origin in the image and its slope toward the  $x$ -axis. Ferrari et al. also proposed a different approach using Gabor wavelets and finding the pectoral muscle boundary by searching for pixels with opposite phase orientation. A part of the procedure that needs to be performed accurately is detection of the correct candidate for the pectoral muscle from several possible edges obtained after filtering with Gabor filters at multiple scales. To test the proposed methods, Ferrari et al. used 84 mammograms from the mini-MIAS database. The FP and FN rates for the method based on the Hough transform and estimation of a straight line to fit the edges of the pectoral muscle were  $1.98 \pm 6.09 \%$  and  $25.19 \pm 19.14 \%$ , respectively. The FP and FN rates for the method based on the Gabor filter were  $0.58 \pm 4.11 \%$  and  $5.77 \pm 4.83 \%$ , respectively. Since the edge of the pectoral muscle often has some curvature, it is not possible to obtain good segmentation by approximating its edge with a straight line.

Kwok et al. [27] addressed the problem of detection of the pectoral muscle using straight line estimation and iterative cliff detection along the straight line. One of the common initial steps is to define an ROI where the pectoral muscle is expected to exist in the given image. Such ROIs are usually defined at the top left corner of the image after the mammogram is oriented as shown in Fig. 14.

After thresholding, Kwok et al. [27] used the Hough transform to detect the “strongest” straight line that also met certain criteria. The cliff detection process was performed along the straight line but not limited to the ROI, because the ROI could be smaller than the actual pectoral muscle as shown in Fig. 14. The edge was defined as the point of inflection in the direction perpendicular to the straight-line estimate of the edge of the pectoral muscle. To test their method, Kwok et al. used the entire MIAS database containing 322 images, with the mammograms relatively small in pixel size due to downsampling to  $400 \mu\text{m}/\text{pixel}$ . After comprehensive evaluation of segmentation accuracy by two radiologists, the results of segmentation using the straight-line estimation method were considered to be good in far fewer cases than for the method of cliff detection. Refinement with the cliff detection method, which was time-consuming, was considered to give good segmentation accuracy in  $88.8 \%$  of the cases by the first radiologist and in  $80.1 \%$  of the cases by the second radiologist.

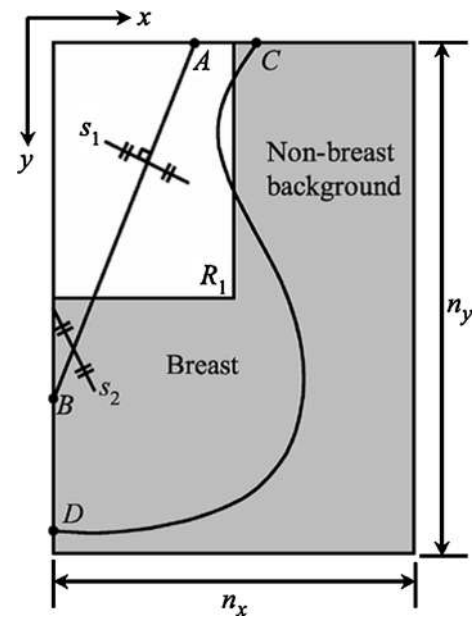


**Fig. 14** Definition of the ROI for the pectoral muscle detection by Kwok et al. [27]

Besides segmentation of breast tissue, Raba et al. [44] also studied segmentation of the pectoral muscle using a region growing algorithm. A problem that arises with the region growing approach is the determination of the correct stopping condition and selection of an appropriate seed point. To avoid false segmentation, Raba et al. applied a size restriction. After the detection process, they used morphological operations to smooth the detected boundary and tested the method on the mini-MIAS database. Their method resulted in  $86 \%$  of good extraction of the pectoral muscle, but no information was provided about the segmentation accuracy and validation of the results.

A method for segmentation of the pectoral muscle by computing an optimal threshold in combination with the Hough transform and polyline fitting was presented by Xu et al. [64]. After finding a suitable threshold, they extracted points from the initial pectoral muscle mask and used the zonal Hough transform. The zonal Hough transform gives the output in the Hough space, from which it is easy to detect the orientation of the line that is close to the straight line that fits the edge of the pectoral muscle. To refine the detected boundary, they used a method of approaching the actual boundary based on the elastic thread. Testing of the proposed method was performed on 60 mammograms that are not publicly available; the results indicated 49 accurately detected of 52 which contained the pectoral muscle and two falsely detected of eight with no visible pectoral muscle. The average percentage of area of overlap with the hand-drawn segmentation masks was  $94.5 \%$ .

Mirzaalian et al. [35] proposed a method for segmentation of the pectoral muscle using a nonlinear diffusion filter. The nonlinear filter is expected to provide good results in noise removal and homogenizing tissue patterns without affecting the sharpness of edges, such as the edge of the pectoral muscle. For testing of their method, Mirzaalian et al. used 90 mammograms from the MIAS database, no information on the selection of the images. They compared their method with methods based on the Hough transform and Gabor wavelets, and demonstrated better results in terms of the mean error and variance of the Hausdorff distance [23]. Mirzaalian et al. [36] also developed a method to extract the breast boundary, for which they used convolution filtering with a low-pass filter that acts as an integrator. The largest region was extracted from a binary image obtained by applying a threshold selected at the knee of the cumulative histogram of the resulting image.

A study on segmentation of the breast tissue from the background and the pectoral muscle from the breast tissue using two methods was presented by Adel et al. [3]. They used Markov random fields and Bayesian segmentation. Their aim was to segment different tissue types that have different but similar gray-level intensities from other areas in the image, which can be either background or a different type of tissue. To group similar tissue types, they relied on interconnectivity of the same tissue by means of the eight-point nearest-neighbor system. Their method, however, did not produce results which could be used in a CAD system because only 68 % of the results of segmentation were rated as good with a test set of 50 mammograms from the mini-MIAS database.

Graph theory methods for identifying the pectoral muscle were presented by Ma et al. [30]. The adaptive pyramids' method uses the assumption that the pectoral muscle is located in the top left corner of a registered mammogram and a set of empirically defined variables to create an image of possible edges. The edges are represented by a sudden change in intensity of neighboring pixels in the mammogram. The minimum spanning trees' method calculates the strongest detected edge. After the edge detection step, Ma et al. used active contours to refine the detected edge because graph-based methods failed to provide accurate segmentation. Both of these methods use several empirically assigned values which were not clearly explained; furthermore, no information was provided about the computational time needed to achieve segmentation of a mammogram. The methods were tested on the same set of 84 mammograms from the mini-MIAS database used by Ferrari et al. [17]. The test results of Ma et al. show slightly worse performance when compared with those of Ferrari et al. in terms of FP and FN measures.

Wongthanavas and Tanvoraphonkchai [63] proposed the use of two-dimensional cellular automata for

segmentation of mammograms. First, they used Otsu's algorithm for initial segmentation of a given mammogram into four different intensity regions in which they were able to detect edges that should correspond well to different tissue types. This method relies on detection of the pectoral muscle no matter where the muscle is situated in the given image. However, the question of accurate segmentation arises because the only method used for border extraction is Otsu's method of thresholding. This method can face difficulties in performing accurate segmentation with low-contrast images as with dense breasts. The method was tested on 84 mini-MIAS mammograms Ferrari et al. [17] with poor performance in segmentation accuracy.

Kinoshita et al. [25] used a Radon-domain method for detection of the nipple and the pectoral muscle. Radon-domain detection is comparable to the Hough transform, which is a commonly used tool for detecting straight lines in images. Each point in the Radon domain corresponds to the integration of the image along a straight line in the spatial domain of the image. Before applying the Radon transform and detection of key points, Kinoshita et al. used the Wiener filter [18] to restore images degraded by noise. On the filtered mammograms, a threshold was applied and background objects were removed using morphological opening and closing operations. After segmenting the breast tissue from the background, without refinement of the boundary, they proceeded with the detection of the pectoral muscle, which was characterized as a bright object with high density. For edge detection, they used the Canny edge detector [8], and on the resulting image, they applied the Radon transform. In the Radon domain, they developed a procedure to detect straight lines that would be suitable candidates to represent the pectoral muscle border by having the slope toward the  $x$ -axis in range between  $5^\circ$  and  $50^\circ$ . Kinoshita et al. did not apply any method for refinement of the detected pectoral muscle edge, which was estimated as a straight line. The method for pectoral muscle detection was tested on a large set of mammograms containing 1080 images, and the resulting FP and FN rates were  $8.99 \pm 38.72\%$  and  $9.13 \pm 11.87\%$ . Kinoshita et al. also presented a method for detection of the nipple using morphological top-hat filtering and characteristics of breast anatomy. The procedure provided good results in cases when the nipple is visible in the segmented image and is located outside of the breast profile.

Tzikopoulos et al. presented a method for segmentation of the pectoral muscle [54] combining two approaches mentioned often, straight-line estimation and validation followed by iterative cliff detection. Iterative cliff detection is used to refine the pectoral muscle boundary detected as a straight line, which may not have adequate accuracy for applications. Although Tzikopoulos et al. mention that tests were carried out using the mini-MIAS database, they

do not provide quantitative analysis of the success of their method in segmentation of the pectoral muscle.

Saltanat et al. [47] used a pixel-value-based mapping scheme for segmentation of the pectoral muscle in mammograms. After preprocessing, they used morphological opening and closing operations in gray scale to sharpen the boundary of regions and obtain a lower number of discrete intensities. By assuming the position of the pectoral muscle to be in the top left corner of the mammogram, they used a region growing method to extract the related area with different stopping conditions. For testing, they used mammograms from the mini-MIAS database and obtained 84 and 92 % of acceptable segmentation according to two different radiologists.

Nagi et al. [39] presented a method for segmentation of both the breast tissue and the pectoral muscle in mammograms. The proposed method uses empirical threshold estimation to create a binary mask of the breast tissue and embedded MATLAB functions in the image processing toolbox, most of them related to black and white morphology, for the removal of background artifacts in the binary image. To segment the pectoral muscle, they used seeded region growing combined with linear contrast enhancement applied to the entire image. Even though the region growing method provides accurate segmentation in cases of good overall contrast between the segmented object and the background, Nagi et al. used a straight-line estimate of the pectoral muscle. The accuracy of estimation of the straight line was not high in some cases; no numerical evaluation of the performance of the proposed method was provided.

A method for detection of the pectoral muscle based on the Markov model was proposed by Wang et al. [56]. The Markov property is a conditional independence of the future evolution based on the past, which means that the whole history of the process is being summarized in the current state. The algorithm observes one row of the image at which the contrast between the pectoral muscle and the background tissue is high, and creates a scan of pixel values along the selected line. The edge is defined as the point with highest standard deviation. This procedure is iterated for all rows where pectoral muscle can be visible. By that, an approximate pectoral muscle boundary is created as a set of pixels with the highest standard deviation in each row of the image. The next step of the proposed method is boundary refinement, for which they used an energy minimization function from an active contour model. This step is expected to provide a smooth boundary without the need for median filtering, which could distort fine edges. The algorithm was tested on 200 mammograms from the DDSM database. Wang et al. achieved 84 % of acceptable segmentation; by using the boundary refinement operation, the acceptable segmentation results rose to 91 %.

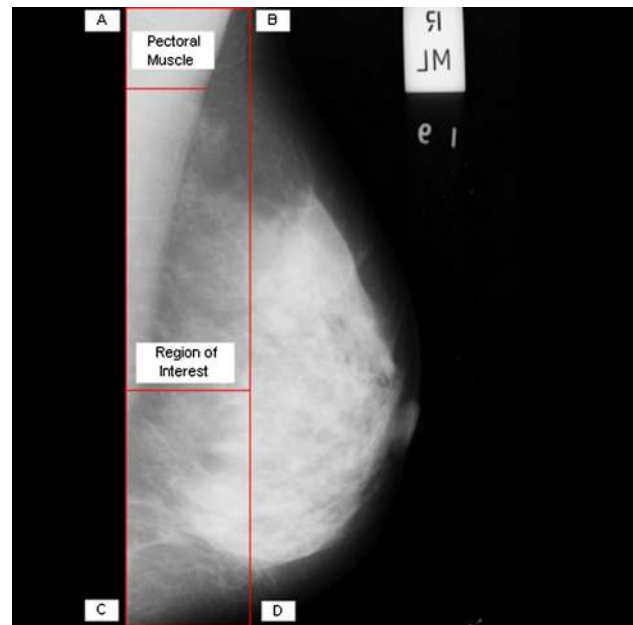


**Fig. 15** ROI for the pectoral muscle segmentation [6]

Tayel and Mohsen [53] proposed an intensity-based segmentation method which detects the pectoral muscle by checking whether the intensity in the top left corner of an image is higher than the mean intensity of pixels belonging to the breast tissue. Pixels belonging to the pectoral muscle are expected to have intensity higher than  $(\text{mean} + \text{standard deviation} * 2/3)$ . The proposed method was tested on the mini-MIAS database and other unspecified mammograms, but no numerical results about the performance of the method were provided; it was claimed that the method performed better than that of Tzikopoulos et al. [54].

Camilus et al. [6] presented a method for extraction of the pectoral muscle based on graph-cut image segmentation and evaluation of the Bezier curve for smoothing the edge obtained by segmentation. Like most of the other methods described in this review, this approach also uses a priori delineation of the ROI where the pectoral muscle is expected to be present. Camilus et al. did not limit the ROI vertically so that it extends through the entire height of the image, as shown in Fig. 15. From the extracted ROI, Camilus et al. created a graph from which they detected multiple boundaries based on various thresholds. To refine the detected boundary, they used points on the detected boundary and fitted a Bezier curve. With a set of 84 randomly chosen mammograms from the mini-MIAS database, they obtained  $FP = 0.0064$  and  $FN = 0.0558$ . Camilus et al. [17] used the same number of images but not the same images as.

The mean-shift segmentation method for segmentation of the pectoral muscle was presented by Sultana et al. [51].

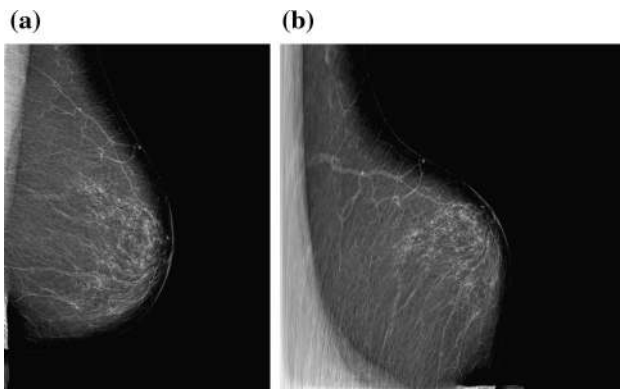


**Fig. 16** **a** MLO image; **b** MLO image after transformation to polar coordinates [9]

The mean-shift segmentation method tries to allocate each pixel from the observed image to clusters by analyzing the pixel's surrounding. To determine whether the observed pixel belongs to a certain cluster, it is necessary to calculate its similarity to other pixels by using a kernel function. Sultana et al. used the Gaussian kernel with the standard deviation value  $\sigma = 6$ . The method was tested on the mini-MIAS database and produced results of 84 % TP rate with the average of 13 % FP rate per image.

Cardoso et al. [9] proposed a graph-cut technique-based method which uses transformation of the image to polar coordinates, Fig. 16. To the image in polar coordinates, they applied a gradient model based on the Prewitt operator. The proposed method was tested on 50 images from the DDSM database and 100 mammograms collected from a local hospital. To evaluate the performance of the method, they used normalized Hausdorff and mean distances, achieving average results of 0.14 and 0.05, respectively. The mean distance between detected and actual pixels which represent the muscle boundary was normalized by the number of pixels belonging to the diagonal of the observed image. The Hausdorff distance is defined as

$$H(A, B) = \max(h(A, B), h(A, B)), \quad (5)$$

where  $A$  and  $B$  represent the sets of the pixels in the reference muscle contour and the segmented muscle contour, respectively, and

$$h(A, B) = \max_{a \in A} \min_{b \in B} \|a - b\|, \quad (6)$$

where  $A$  and  $B$  are two contours or sets of points to be compared.

The same group of authors proposed a similar approach for detection of the pectoral muscle in [15]. Strictly from the image processing point of view, these two papers use the same methodology; the difference is in the classification process, where they use support vector machine (SVM) to

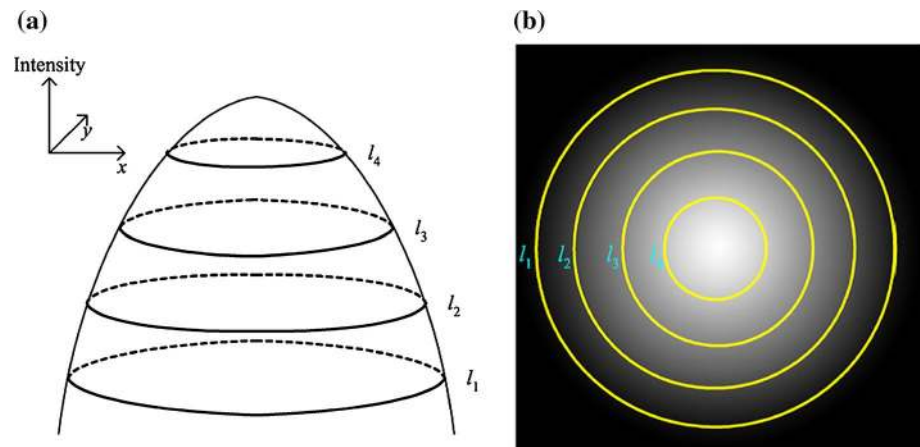
achieve better selection of the pectoral muscle's end points in the horizontal and vertical axis, and thereby reduce FP and FN errors. The use of an SVM classifier and a training set of images improved the accuracy of the proposed method by one order of magnitude according to Hausdorff and mean distance metrics.

Subashini et al. [49] proposed a method for detection of masses in digital mammograms using connected component labeling. This method also incorporates preprocessing steps which include detection of the breast boundary and removal of the pectoral muscle. For breast boundary detection, they used simple thresholding with fixed thresholds. Pectoral muscle detection was handled in a more complex manner. The first step in the pectoral muscle detection process was isolating the ROI where the entire pectoral muscle is situated. On the isolated ROI, they applied thresholding and scanned the obtained binary image to segment the pectoral muscle. No information is provided about the success of the proposed method in terms of segmentation accuracy. It could be expected that global thresholding will not provide accurate results because mammograms vary substantially in intensities of the corresponding tissues. Furthermore, Subashini et al. did not include any step for refinement of the detected boundary.

Bandyopadhyay [5] presented a work that deals with segmentation of mammograms and regions within a mammogram. This paper lacks a clear explanation of the method, which does not segment the pectoral muscle from the breast image but only tries to denote the ROI in MLO mammograms where the pectoral muscle should be present. Unlike most of the other published methods for this purpose in which the ROIs used are rectangular in shape, this approach defines a triangular ROI by selecting key points in the image. The point that is difficult to detect is related to the width of the breast tissue at the upper edge of the mammogram. The proposed method is suitable for square images, such as the images from the mini-MIAS database, and may not provide good results for images of different aspect ratios and different distances of the breast tissue from the left edge of the image. Because mammograms in the mini-MIAS database are not provided according to the DICOM standard, their positioning and aspect ratio should not be considered when developing a robust preprocessing method in a CAD system.

Hong and Sohn [22] presented a topographic approach for segmentation of objects in mammograms, such as masses. They aimed at segmentation of salient regions, which are defined as regions that appear distinctively against the surrounding background. In a mammogram, the salient regions are the breast region and the pectoral muscle, because they appear brighter than the remaining part of the image which can be treated as the background in both cases. To be able to select objects of similar intensity, Hong

**Fig. 17** Illustration of the image model from [22]. **a** Surface model of the image and the levels of *gray* values to quantize; **b** isocontours superimposed on the image with given levels of *gray* values to quantize MLO image [22]



and Sohn aimed at building isointensity contour maps which represent pixels of the same intensity joined together to form objects. An example of an isointensity contour map of an image with intensity varying in relation to distance from the origin is shown in Fig. 17.

The method of Hong and Sohn was aimed mainly at segmentation of masses in mammograms, and therefore, no numerical results of accuracy in the detection of pectoral muscles were provided. However, the results in the detection of masses were good, and the authors claimed 100 % detection rate with 3.8 FP detection per image on the average with a set of 400 mammograms from the DDSM. While these results may imply that detection of the pectoral muscle was successful, the accuracy of detecting the actual border needs to be analyzed.

Maitra et al. [31] dealt with the segmentation of mammograms to detect abnormal masses using the binary homogeneity enhancement algorithm. Their first step is running the binary homogeneity enhancement algorithm, which is used to group pixels in a small number of clusters according to their difference with respect to the neighboring pixel in a row. Pixels for which the difference is below the chosen maximum difference threshold belong to the same cluster. After this step, they proceeded to the edge detection step by detecting edges of clusters containing pixels with the same intensity. From the presented results, it is seen that this approach does not give a smooth segmentation line for the pectoral muscle even in images where there is a large difference in intensity between the pectoral muscle and the breast tissue. Maitra et al. tested the performance of their method on the mini-MIAS database and reported a high accuracy of 0.9987, which do not appear to agree with visual inspection of the results shown in their paper. No information was provided about the ground truth used; the mini-MIAS database does not provide segmentation masks for breast tissue regions and pectoral muscles. A similar work from the same group of authors can be found in Ref. [32].

Czaplicka and Włodarczyk [13] proposed a method for skin-line estimation and pectoral muscle segmentation which uses iterative thresholding and refinement of initial segmentation by linear regression. To test the method, they relied on 300 mammograms from the mini-MIAS database and reported accurate segmentation in 98 % of cases; however, the information provided on the experimental methodology and ground truth is not complete.

Camilus et al. [7] proposed an improved approach for detection of the pectoral muscle as compared to their earlier work [6]. In the improved work, they used the watershed transform of the ROI where the pectoral muscle is expected to be situated. By performing the watershed transformation, which is sensitive to the local minimum, the resulting image should contain one line which represents the pectoral muscle, stretching from the top of the image toward the left and creating a triangular shape, as shown in Fig. 18. From this line, it is possible to estimate a curve which can be used as the boundary of the pectoral muscle. The proposed method was tested on 84 mammograms from the mini-MIAS database and resulted in good-quality segmentation in 94 % of the mammograms.

Chen and Zwiggelaar [12] addressed segmentation of the pectoral muscle by using a region growing method with the seed point located close to the border of the pectoral muscle and the breast tissue. To refine the detected boundary, they used locally weighted scatter-plot smoothing, which is a locally weighted regression-based method. To test the accuracy of the proposed method, they used 321 mammograms from the mini-MIAS database and 248 mammograms from the EPIC database [14]. The results for the mini-MIAS database in the categories of accurate, nearly accurate, acceptable, and unacceptable segmentation were 67.9, 24.9, 5.0, and 2.2 %, respectively, and for the EPIC database 62.5, 25.4, 5.6, and 6.5 %, respectively.

A method for detection of the pectoral muscle which uses an average gradient and a shape-based feature was presented by Chakraborty et al. [11]. The proposed method

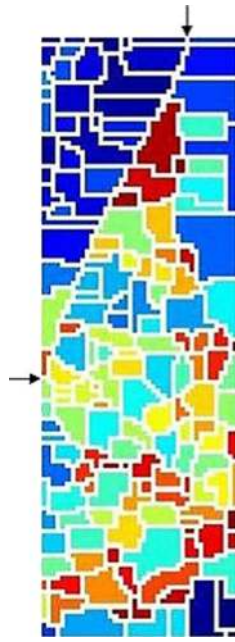


**Fig. 18** Watershed transformation of mdb043 from the mini-MIAS database where the pectoral muscle segmentation line is denoted by arrows [7]

consists of straight-line approximation of the pectoral muscle boundary and smooth boundary detection around the approximated straight line. Detection of the pectoral muscle edge usually proves to be more difficult in the area close to the left edge of the mammogram if the breast tissue is oriented such that the pectoral muscle is situated in the top left corner of the image. The reason for this observation is that the pectoral muscle attenuates X-rays more than the rest of the breast tissue and it is thicker in the area that is being imaged in the top left corner. For this reason, Chakraborty et al. decided to use a straight-line estimation based on pixels that are situated close to the top of the mammogram. Smooth boundary detection was carried along the estimated straight line to allow more precise segmentation in cases of muscle curvature. The proposed method was tested on 80 images from the mini-MIAS database, 80 digital radiography (DR) mammograms, and 40 computed radiography (CR) mammograms. The percentages of mismatched pixels for each of the three image datasets were reported as  $10.92\% \pm 17.07\%$ ,  $10.75\% \pm 14.20\%$ , and  $23.38\% \pm 40.92\%$ , respectively.

Abdellatif et al. [1] dealt with segmentation of the pectoral muscle using the graph-cut technique and muscle edge estimation using the Bezier curve. The graph-cut technique is used to detect the edge of the muscle which is represented by a sudden change in intensity. The proposed method uses eigenvector calculation to find the cut that corresponds best to the pectoral muscle. Since the edge of the

segmented muscle is not smooth, Abdellatif et al. proposed use of the Bezier curve, which can vary from a straight line to an arbitrary curved segment. The segmentation method was tested on 80 mammograms from the mini-MIAS database, and results were compared against segmentation achieved using the Hough transform. The proposed method achieved decreases in FP of 0.012 and in FN of 0.204.

Li et al. [29] presented an approach to segmentation of the pectoral muscle based on texture analysis and difference in intensity by. They also used positioning of the mammogram such that the pectoral muscle is situated in the top left corner and the property of the muscle being relatively homogenous with high variation in the intensity in the muscle border area. From the original image, they constructed two likelihood maps, in the texture field and in the intensity field. By combining these two maps and searching for the corresponding maxima, they obtained a ragged edge of the pectoral muscle, which was treated as the sum of the true edge and noise. To smooth the edge, they used the Kalman filter. The Kalman filter was employed to refine the initial edge by modeling it as an accelerated displacement curve. The approach was expected to differentiate between correctly and erroneously chosen edge pixels by checking whether the edge distance from the left border is increasing or decreasing when moving from the top of the image toward the bottom. They tested the proposed method on the entire mini-MIAS database and 100 mammograms from the DDSM, and obtained 90.06 and 92 % correct segmentation, respectively.

Maitra et al. [33] proposed a method which uses estimation of the pectoral muscle position in mammograms and further analysis of the ROI. Their aim was to find a suitable pixel for use as the seed for a region growing step, which was modified to detect edge of the region in the top left corner. The method achieved 308 acceptable segmentation results out of 322 mammograms from the mini-MIAS database.

Shanmugavadivu and Sivakumar [48] used a fractal method to segment the pectoral muscle in mammograms. As the first step, they applied contrast enhancement, followed by edge detection using the Sobel operator. By knowing the expected muscle position and by comparing the detected pixels with the calculated fractal dimension of the image, they managed to segment the pectoral muscle area. No information was provided about the success of the proposed method, and only two examples of segmentation for mammograms from the mini-MIAS database were shown in the paper. No edge refinement is included in their method.

Mustra and Grgic [37] presented a combined approach for pectoral muscle segmentation. They also relied on extracting an ROI and contrast enhancement using CLAHE, after which they selected 10 points from the



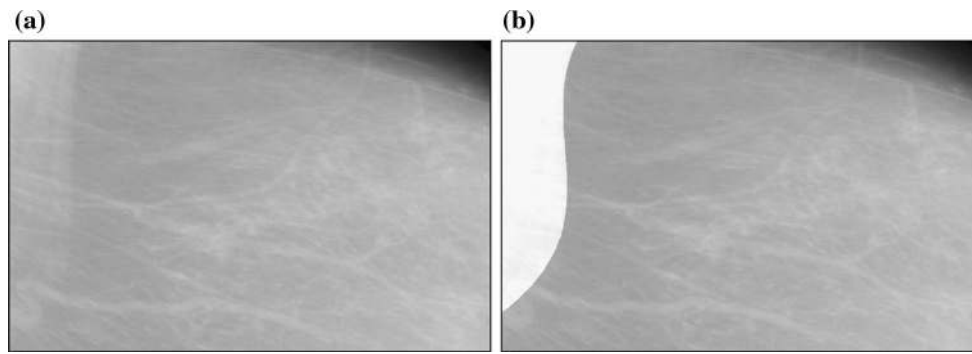


**Fig. 19** **a** Original ROI for the pectoral muscle detection; and **b** result of the pectoral muscle segmentation for “mdb151” [37]

thresholded ROI. The selected points were used for polynomial fitting of the segmentation curve, which is represented as a third-degree polynomial. This approach provides good segmentation accuracy in cases of low contrast of the pectoral muscle toward the breast tissue. Even though polynomial estimation introduces some error in segmentation accuracy, it has the ability of tracking the actual muscle boundary accurately. Figure 19 shows segmentation using the proposed method of a “difficult” image from the mini-MIAS database, where polynomial estimation of the pectoral muscle edge gives an acceptable result and threshold-based segmentation would fail.

The results of the proposed method indicated 96.6 % of accurate segmentation over all 322 mammograms from the mini-MIAS database.

#### 4 Comparison of segmentation approaches

In the preceding sections, we have reviewed recent publications on segmentation of the breast tissue from the background and the pectoral muscle from the breast tissue. This section summarizes the various approaches so that overlaps between them are demonstrated; the discussion will also show which approaches give good results in terms of segmentation accuracy. Since most of the proposed methods were tested on mini-MIAS and DDSM images, it will be possible to present a valid comparison. Differences in segmentation accuracy are largely influenced by the quality of the images used for testing; therefore, it would be best if one could test all of the algorithms using exactly the same image set. Since segmentation of the breast tissue from the background and segmentation of the pectoral muscle from the breast tissue have significant differences in background from which objects are segmented, there is a significant difference in segmentation approaches. For segmentation of the breast tissue, authors mostly use intensity-based and gradient methods because of higher contrast to the background while segmentation of the pectoral muscle from the

breast tissue relies more on image preprocessing for contrast enhancements and estimation of the pectoral muscle boundary. The methods reviewed in the preceding sections can be grouped according to the approaches used and their success as shown in Table 1.

Automatic detection of the pectoral muscle has been achieved using many different approaches. The most commonly used approach uses straight-line estimation to approximate the pectoral muscle edge or to define the ROI where an algorithm should search for the pectoral muscle. Straight lines in an image, after initial segmentation, are easily detected using the Hough transform, which is the most commonly used tool for straight-line estimation. Region growing techniques give more precise segmentation results, especially when pectoral muscles have curvature. However, region growing does not always give a good segmentation result because of the stopping condition which cannot be automatically tuned for each image. To overcome those problems, many researchers have relied on placing the seed point somewhere on the actual pectoral muscle boundary; this is because the boundary area has the largest variation in local contrast and proper selection of a seed pixel can prevent false segmentation. Pectoral muscles are not always clearly visible in mammograms, especially of dense breasts, because of poor contrast. To prevent false segmentation in mammograms with poor contrast, Mustra and Grgic [37] proposed polynomial fitting of the detected edge to ensure that the detected pectoral muscle satisfies some criteria according to the part of the muscle which has good contrast and is clearly visible. Table 2 lists various published approaches to segmentation of the pectoral muscle, the datasets used for testing, and the accuracy of the results.

Generally, we can say that the raw image quality has a significant influence on the segmentation results in case of the breast boundary detection as well as in the pectoral muscle segmentation. Some improvement in terms of accurately segmented images from a specific dataset is shown in most of newly presented papers, but accuracy of

**Table 1** Breast boundary segmentation methods according to the approaches used with accuracy of each method

Segmentation approach	Method proposed by	Dataset used	Segmentation accuracy
Thresholding	Wei et al. [57]	DDSM	94.9 %
	Raba et al. [44]	MIAS	98 %
	Mustra et al. [38]	KBD-FER	100 %
	Tayel and Mohsen [53]	mini-MIAS	N/A
	Maitra et al. [33]	mini-MIAS	95.71 %
	Mustra and Grgic [37]	mini-MIAS	99.1 % successful
	Czaplicka and Włodarczyk [13]	300 mini-MIAS	98 %
Morphology	Wei et al. [57]	DDSM	94.9 %
	Yapa and Harada [65]	mini-MIAS (100 images)	98.6 and 99.1 % completeness and correctness
	Zhang et al. [66]	mini-MIAS (20 images)	N/A
Region growing	Raba et al. [44]	mini-MIAS	98 %
	Zhang et al. [66]	mini-MIAS (20 images)	N/A
	Chen and Zwiggelaar [12]	mini-MIAS EPIC	98.8 % accurate and 1.2 % inaccurate 91.5 % accurate and 8.5 % inaccurate
Active contours	Wirth and Stapinski [60]	MIAS (25 images)	3 % of error in segmentation based on pixel number
	Ferrari et al. [16]	MIAS (84 images)	FP = $0.41 \pm 0.25$ % and FN = $0.58 \pm 0.67$ %. 0.96 completeness and correctness
	Martí et al. [34]	MIAS (65 images)	mean correctness $0.9697 \pm 0.0507$ and completeness $0.9547 \pm 0.0618$
		DDSM (24 images)	mean correctness $0.9524 \pm 0.0557$ and completeness $0.9744 \pm 0.0103$
Thresholding and Gabor filters	Casti et al. [10]	mini-MIAS and FFDM	99.87 % $\pm$ 0.003 % completeness 99.57 % $\pm$ 0.004 % correctness 99.37 % $\pm$ 0.005 % quality

automatic segmentation methods is still couple of percent below 100 %. Uncontrolled environments will surely give even worse results in terms of the segmentation successfulness. It is almost impossible to create a numeric rule which would measure the acceptable segmentation accuracy, and for now we have to only rely on testing in real-world environments. A general rule of satisfying segmentation performance can be set at around 95 % for both the breast boundary detection and the pectoral muscle segmentation algorithms.

## 5 Conclusions

In this paper, we have presented a review of several published works on the development of automatic methods for segmentation of the breast tissue and the pectoral muscle regions in scanned SFM and FFDM images. Work in this field dates from the beginning of the development of digital image processing algorithms for medical images in the 1980s, and many different approaches have evolved from then on. The majority of papers referenced in this review is from the last 10 years and show

examples of streaming of segmentation techniques in similar directions, influenced mainly by the development of computational capability. Modern medical imaging systems incorporate many image processing methods which are used to improve image quality, and many additional tools are at the disposal of the radiologist. Mammography, together with other imaging modalities, has shifted toward digital technology because of the advantages it offers, especially in storage and postprocessing. For presentation and processing applications, mammography workstations need to incorporate accurate and fast segmentation methods together with contrast enhancement methods to provide better visibility of important details and reduce false-negative results. Among the most widely used approaches for scanned images is intensity-based thresholding combined with morphological operations for removing background objects and segmenting pixels which belong to the breast tissue. Further refinement of the segmented breast boundary is achieved mostly with local contrast enhancement and subdivision of the image to obtain a more precise threshold and smoother boundary. These approaches work well on both FFDM and SFM images.

**Table 2** Pectoral muscle segmentation methods according to the approaches used with accuracy of each method

Segmentation approach	Method proposed by	Dataset used	Segmentation accuracy
Straight-line estimation	Kwok et al. [26]	MIAS	94 %
	Ferrari et al. [17]	MIAS	FP = 1.98 ± 6.09 % and FN = 25.19 ± 19.14 %
	Kwok et al. [27]	MIAS	Straight line 75.5 % and 62.8 % for two radiologists, curve approximation 88.8 % and 80.1 % for two radiologists
	Xu et al. [64]	60	Detection precision of 49/52 and false- positive rate of 2/8
	Kinoshita et al. [25]	1080 images	FP = 8.99 ± 38.72 % and FN = 9.13 ± 11.87 %
	Tzikopoulos et al. [54]	mini-MIAS	N/A
	Chakraborty et al. [11]	80 mini-MIAS, 80 DR mammograms and 40 CR mammograms	10.92 % ± 17.07 %, 10.75 % ± 14.20 %, and 23.38 % ± 40.92 % mismatched pixels, respectively
Thresholding	Weidong and Shunren [59]	60 mammograms	81.7 %
	Subashini et al. [49]	300 mini-MIAS	N/A
	Czaplicka and Włodarczyk [13]		98 %
Region growing	Raba et al. [44]	mini-MIAS	98 %
	Zhang et al. [66]	mini-MIAS (20 images)	N/A
	Chen and Zwiggelaar [12]	mini-MIAS and EPIC	92.8 and 87.9 %
	Saltanat et al. [47]	mini-MIAS	92 %
	Nagi et al. [39]	mini-MIAS and private dataset	N/A
	Maitra et al. [33]	mini-MIAS	95.7 %
Wavelet	Mustra et al. [38]	KBD-FER	85 %
	Ferrari et al. [17]	MIAS	FP = 0.58 ± 4.11 % and FN = 5.77 ± 4.83 %
	Mirzaalian et al. [35]	MIAS (90 images)	Hausdorff distance measure: 14.7585 ± 7.7737 Mean of absolute error distance measure: 2.5525 ± 1.6343
Markov random fields	Adel et al. [3]	mini-MIAS (50 images)	68 %
	Wang et al. [56]	mini-MIAS (200 images)	84 %
Polynomial fit	Mustra and Grgic [37]	mini-MIAS	96.6 %

Regarding detection of the pectoral muscle, there have been many different approaches due to the need of overcoming low contrast of the pectoral muscle toward rest of the breast tissue. Most of the proposed methods use straight-line estimation, usually provided by the Hough transform, and further refinement of the detected boundary. To achieve precise segmentation, some researchers have relied on the region growing method with a special placement of the seed point. The seed point is best placed somewhere on the actual pectoral muscle boundary to prevent problems related to the stopping condition.

To test the results of segmentation of both breast tissue and pectoral muscle regions, most researchers have used both the (mini)-MIAS and the DDSM images, which are publicly available. Using the same images for testing of different methods is essential for comparison of the results;

however, both of these datasets are outdated and consist of scanned SFMs. The results obtained from various proposed methods and algorithms show good segmentation accuracy in more than 95 % of cases when considering breast tissue segmentation and more than 90 % when considering segmentation of the pectoral muscle.

Even though the segmentation results reported in the literature appear to be good, there is still the need to design and implement methods for a completely automated and robust method which will provide high accuracy in a consistent manner across mammographic images of several types. Besides the X-ray breast imaging, there are also other techniques which prove to be better and less harmful in many cases such as MRI, ultrasound, and thermography. Images obtained with different imaging technologies will have significantly different properties, and different

segmentation methods will have to be applied to achieve good and clinically applicable results.

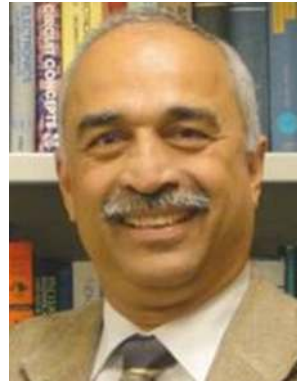
## References

- Abdellatif H, Taha TE, Zahran OF, Al-Nauimy W, El-Samie FA (2012) Automatic pectoral muscle boundary detection in mammograms using eigenvectors segmentation. In: 29th national radio science conference. IEEE, pp 633–640
- ACR (2003) American College of Radiology Breast Imaging Reporting and Data System (BI-RADS). American College of Radiology
- Adel M, Rasigni M, Bourennane S, Juhan V (2007) Statistical segmentation of regions of interest on a mammographic image. *EURASIP J Adv Signal Process* 2:1–8. doi:10.1155/2007/49482
- Baker JA, Rosen EL, Crockett MM, Lo JY (2005) Accuracy of segmentation of a commercial computer-aided detection system for mammography. *Radiology* 235(2):385–390. doi:10.1148/radiol.2352040899
- Bandyopadhyay SK (2010) Pre-processing of mammogram images. *Int J Eng Sci Technol* 2(11):6753–6758
- Camilus KS, Govindan VK, Sathidevi PS (2010) Computer-aided identification of the pectoral muscle in digitized mammograms. *J Digit Imaging* 23(5):562–580. doi:10.1007/s10278-009-9240-6
- Camilus KS, Govindan VK, Sathidevi PS (2011) Pectoral muscle identification in mammograms. *J Appl Clin Med Phys Am Coll Med Phys* 12(3):3285
- Canny J (1986) A computational approach to edge detection. *Pattern. IEEE Trans Pattern Anal Mach Intell* 6:679–698
- Cardoso JS, Domingues I, Amaral I, Moreira I, Passarinho P, Santa Comba J, Correia R, Cardoso MJ (2010) Pectoral muscle detection in mammograms based on polar coordinates and the shortest path. In: 2010 annual international conference of the IEEE Engineering in Medicine and Biology Society (EMBC). IEEE, pp 4781–4784
- Casti P, Mencattini A, Salmeri M, Ancona A, Mangeri F, Pepe ML, Rangayyan RM (2013) Estimation of the breast skin-line in mammograms using multidirectional Gabor filters. *Comput Biol Med* 43(11):1870–1881. doi:10.1016/j.combiomed.2013.09.001
- Chakraborty J, Mukhopadhyay S, Singla V, Khandelwal N, Bhattacharyya P (2012) Automatic detection of pectoral muscle using average gradient and shape based feature. *J Digit Imaging* 25(3):387–399. doi:10.1007/s10278-011-9421-y
- Chen Z, Zwiggleaar R (2012) A combined method for automatic identification of the breast boundary in mammograms. In: 5th international conference on biomedical engineering and informatics (BMEI). IEEE, pp 121–125
- Czaplicka K, Włodarczyk J (2011) Automatic breast-line and pectoral muscle segmentation. *Schedae Inform* 20:195–209
- Day N, Oakes S, Luben R, Khaw KT, Bingham S, Welch A, Wareham N (1999) EPIC-Norfolk: study design and characteristics of the cohort. *European prospective investigation of cancer. Br J Cancer* 80(Suppl 1):95–103
- Domingues I, Cardoso JS, Amaral I, Moreira I, Passarinho P, Santa Comba J, Correia R, Cardoso MJ (2010) Pectoral muscle detection in mammograms based on the shortest path with endpoints learnt by SVMs. In: Annual international conference of the IEEE Engineering in Medicine and Biology Society. IEEE, pp 3158–3161
- Ferrari RJ, Rangayyan RM, Desautels JEL, Borges RA, Frere AF (2004) Identification of the breast boundary in mammograms using active contour models. *Med Biol Eng Comput* 42(2):201–208. doi:10.1007/Bf02344632
- Ferrari RJ, Rangayyan RM, Desautels JE, Borges RA, Frere AF (2004) Automatic identification of the pectoral muscle in mammograms. *IEEE Trans Med Imaging* 23(2):232–245
- Gonzalez RC, Woods RE (2008) Digital image processing. Pearson Education Inc, Upper Saddle River
- Gonzalez RC, Woods RE, Eddins SL (2009) Digital image processing using MATLAB, vol 2. Gatesmark, Knoxville
- Heath M, Bowyer K, Kopans D, Moore R, Kegelmeyer WP (2001) The digital database for screening mammography. *IWDM 2000*:212–218
- Hong BW, Brady M (2003) A topographic representation for mammogram segmentation. In: Ellis RE, Peters TM (eds) Medical image computing and computer-assisted intervention-MICCAI. Springer, Berlin, Heidelberg, pp 730–737
- Hong BW, Sohn BS (2010) Segmentation of regions of interest in mammograms in a topographic approach. *IEEE Trans Inform Technol Biomed* 14(1):129–139. doi:10.1109/TITB.2009.2033269
- Huttenlocher DP, Klanderman GA, Rucklidge WJ (1993) Comparing Images Using the Hausdorff Distance. *IEEE Trans Pattern Anal Mach Intell* 15(9):850–863. doi:10.1109/34.232073
- Karnan M, Thangavel K (2007) Automatic detection of the breast border and nipple position on digital mammograms using genetic algorithm for asymmetry approach to detection of microcalcifications. *Comput Methods Programs Biomed* 87(1):12–20. doi:10.1016/j.cmpb.2007.04.007
- Kinoshita SK, Azevedo-Marques PM, Pereira RR Jr, Rodrigues JA, Rangayyan RM (2008) Radon-domain detection of the nipple and the pectoral muscle in mammograms. *J Digit Imaging* 21(1):37–49. doi:10.1007/s10278-007-9035-6
- Kwok SM, Chandrasekhar R, Attikiouzel Y (2001) Automatic pectoral muscle segmentation on mammograms by straight line estimation and cliff detection. In: The seventh Australian and New Zealand intelligent information systems conference. IEEE, pp 67–72
- Kwok SM, Chandrasekhar R, Attikiouzel Y, Rickard MT (2004) Automatic pectoral muscle segmentation on mediolateral oblique view mammograms. *IEEE Trans Med Imaging* 23(9):1129–1140. doi:10.1109/TMI.2004.830529
- Lewin JM, Hendrick RE, D’Orsi CJ, Isaacs PK, Moss LJ, Karellas A, Sisney GA, Kuni CC, Cutter GR (2001) Comparison of full-field digital mammography with screen-film mammography for cancer detection: results of 4,945 paired examinations. *Radiology* 218(3):873–880. doi:10.1148/radiology.218.3.r01mr29873
- Li Y, Chen H, Yang Y, Yang N (2012) Pectoral muscle segmentation in mammograms based on homogenous texture and intensity deviation. *Pattern Recogn* 46:681–691
- Ma F, Bajger M, Slavotinek JP, Bottema MJ (2007) Two graph theory based methods for identifying the pectoral muscle in mammograms. *Pattern Recogn* 40(9):2592–2602. doi:10.1016/j.patcog.2006.12.011
- Maitra I, Nag S, Bandyopadhyay S (2011) Automated digital mammogram segmentation for detection of abnormal masses using binary homogeneity enhancement algorithm. *Indian J Comput Sci Eng* 2(3):416–427
- Maitra IK, Nag S, Bandyopadhyay SK (2011) Detection and isolation of pectoral muscle from digital mammogram: an automated approach. *Int J Adv Res Comput Sci* 2(3):375–380
- Maitra IK, Nag S, Bandyopadhyay SK (2012) Technique for pre-processing of digital mammogram. *Comput Methods Programs Biomed* 107(2):175–188. doi:10.1016/j.cmpb.2011.05.007
- Martí R, Oliver A, Raba D, Freixenet J (2007) Breast skin-line segmentation using contour growing. In: Martí J, Benedí JM, Mendonça AM, Serrat J (eds) Pattern recognition and image analysis. Springer, Berlin, Heidelberg, pp 564–571

35. Mirzaalian H, Ahmadzadeh MR, Sadri S (2007) Pectoral muscle segmentation on digital mammograms by nonlinear diffusion filtering. In: IEEE Pacific Rim conference on communications, computers and signal processing, 2007. IEEE, pp 581–584
36. Mirzaalian H, Ahmadzadeh MR, Sadri S, Jafari M (2007) Pre-processing algorithms on digital mammograms. In: IAPR conference on machine vision applications, Tokyo. MVA, pp 118–121
37. Mustra M, Grgic M (2012) Robust automatic breast and pectoral muscle segmentation from scanned mammograms. *Sig Process* 93(10):2817–2827
38. Mustra M, Bozek J, Grgic M (2009) Breast border extraction and pectoral muscle detection using wavelet decomposition. In: EUROCON 2009. IEEE, pp 1426–1433
39. Nagi J, Abdul Kareem S, Nagi F, Khaleel Ahmed S (2010) Automated breast profile segmentation for ROI detection using digital mammograms. In: IEEE EMBS conference on biomedical engineering and sciences (IECBES). IEEE, pp 87–92
40. NEMA (2011) Digital imaging and communications in medicine (DICOM), Dicom Standard. NEMA Publications, Rosslyn
41. Oliver A, Freixenet J, Marti R, Pont J, Perez E, Denton ER, Zwiggelaar R (2008) A novel breast tissue density classification methodology. *IEEE transactions on information technology in biomedicine: a publication of the IEEE Engineering in Medicine and Biology Society* 12(1):55–65. doi:10.1109/TITB.2007.903514
42. Oliver A, Llado X, Perez E, Pont J, Denton ER, Freixenet J, Marti J (2010) A statistical approach for breast density segmentation. *J Digit Imaging* 23(5):527–537. doi:10.1007/s10278-009-9217-5
43. Qi H, Head JF (2001) Asymmetry analysis using automatic segmentation and classification for breast cancer detection in thermograms. In: Proceedings of the 23rd annual international conference of the IEEE. Engineering in Medicine and Biology Society, pp 2866–2869
44. Raba D, Oliver A, Marti J, Peracaula M, Espunya J (2005) Breast segmentation with pectoral muscle suppression on digital mammograms. *Lect Notes Comput Sc* 3523:471–478
45. Rickard HE, Tourassi GD, Eltonsy N, Elmaghraby AS (2004) Breast segmentation in screening mammograms using multiscale analysis and self-organizing maps. In: 26th annual international conference of the IEEE Engineering in Medicine and Biology Society, 2004. IEEE, pp 1786–1789
46. Saidin N, Ngah UK, Sakim H, Siong DN, Hoe MK (2009) Density based breast segmentation for mammograms using graph cut techniques. In: IEEE region 10 conference TENCON 2009. IEEE, pp 1–5
47. Saltanat N, Hossain MA, Alam MS (2010) An efficient pixel value based mapping scheme to delineate pectoral muscle from mammograms. In: 2010 IEEE fifth international conference on bio-inspired computing: theories and applications. IEEE, pp 1510–1517
48. Shanmugavadivu P, Sivakumar V (2013) Segmentation of pectoral muscle in mammograms using fractal method. In: 2013 international conference on computer communication and informatics (ICCCI). IEEE, pp 1–6
49. Subashini TS, Ramalingam V, Palanivel S (2010) Pectoral muscle removal and detection of masses in digital mammogram using CCL. *Int J Comput Appl* 1(6):66–70
50. Suckling J, Parker J, Dance DR, Astley S, Hutt I, Boggis CRM, Ricketts I, Stamatakis E, Cernaes N, Kok SL, Taylor P, Betal D, Savage J (1994) The mammographic image analysis society digital mammogram database. In: Proceedings of the 2nd international workshop on digital mammography, pp 375–378
51. Sultana A, Ciuc M, Strungaru R (2010) Detection of pectoral muscle in mammograms using a mean-shift segmentation approach. In: 8th international conference on communications. IEEE, pp 165–168
52. Sun YJ, Suri JS, Desautels JEL, Rangayyan RM (2006) A new approach for breast skin-line estimation in mammograms. *Pattern Anal Appl* 9(1):34–47. doi:10.1007/s10044-006-0023-0
53. Tayel M, Mohsen A (2010) Breast boarder boundaries extraction using statistical properties of Mammogram. In: 10th international conference on signal processing (ICSP). IEEE, pp 2468–2471
54. Tzikopoulos S, Georgiou H, Mavroforakis M, Dimitropoulos N, Theodoridis S (2009) A fully automated complete segmentation scheme for mammograms. In: 16th international conference on digital signal processing. IEEE, pp 1–6
55. van Engeland S, Snoeren P, Hendriks J, Karssemeijer N (2003) A comparison of methods for mammogram registration. *IEEE Trans Med Imaging* 22(11):1436–1444. doi:10.1109/TMI.2003.819273
56. Wang L, Zhu ML, Deng LP, Yuan X (2010) Automatic pectoral muscle boundary detection in mammograms based on Markov chain and active contour model. *J Zhejiang Univ Sci C* 11(2):111–118. doi:10.1631/jzus.C0910025
57. Wei K, Guangzhi W, Hui D (2005) Segmentation of the breast region in mammograms using watershed transformation. In: 27th annual international conference of the Engineering in Medicine and Biology Society. IEEE-EMBS, pp 6500–6503
58. Weickert J (1997) A review of nonlinear diffusion filtering. *Scale-Space Theory in Computer Vision* 1252:3–28
59. Weidong X, Shunren X (2003) A model based algorithm to segment the pectoral muscle in mammograms. In: Proceedings of the 2003 international conference on neural networks and signal processing. IEEE, pp 1163–1169
60. Wirth MA, Stapinski A (2003) Segmentation of the breast region in mammograms using active contours. In: Ebrahimi T, Sikora T (eds) Visual communications and image processing. International Society for Optics and Photonics, Lugano, pp 1995–2006
61. Wirth MA, Lyon J, Nikitenko DA (2004) Fuzzy approach to segmenting the breast region in mammograms. In: IEEE annual meeting of the fuzzy information processing NAFIPS'04. IEEE, pp 474–479
62. Wirth M, Lyon J, Fracchini M, Nikitenko D (2004) The effect of mammogram databases on algorithm performance. In: 17th IEEE symposium on computer-based medical systems. IEEE, pp 15–20
63. Wongthanavas S, Tanvoraphonkchai S (2008) Cellular automata-based identification of the pectoral muscle in mammograms. In: The proceedings of the 3rd international symposium on biomedical engineering, pp 294–298
64. Xu W, Li L, Liu W (2007) A novel pectoral muscle segmentation algorithm based on polyline fitting and elastic thread approaching. In: The 1st international conference on bioinformatics and biomedical engineering. IEEE, pp 837–840
65. Yapa RD, Harada K (2008) Breast skin-line estimation and breast segmentation in mammograms using fast-marching method. *International Journal of Biological, Biomedical and Medical Sciences* 3(1):54–62
66. Zhang Z, Lu J, Yip YJ (2010) Automatic segmentation for breast skin-line. In: IEEE 10th international conference on computer and information technology. IEEE, pp 1599–1604
67. Zuiderveld K (1994) Contrast limited adaptive histogram equalization. In: Heckbert PS (ed) Graphics gems IV. Academic Press Professional, Inc, San Diego, pp 474–485



**Mario Mustra** is an Assistant Professor at the University of Zagreb, Croatia. His current research interests are image processing, medical imaging, signal processing, and development of CAD algorithms in mammography.



**Rangaraj M. Rangayyan** is a Professor with the University of Calgary, Canada. His research interests are digital signal and image processing, biomedical signal analysis, medical imaging and image analysis, and computer vision.



**Mislav Grgic** is a Professor at the University of Zagreb, Croatia. His research interests include multimedia communications, digital image, and signal processing. In these fields, he has by now published over 130 scientific papers.